The Opportunity Rover's Athena Science Investigation at Meridiani Planum, Mars

S. W. Squyres, *et al.*

Science **306**, 1698 (2004);
DOI: 10.1126/science.1106171

Science (print ISSN 0036-8075; online ISSN 1095-9203) is published weekly, except the last week in December, by the American Association for the Advancement of Science, 1200 New York Avenue NW, Washington, DC 20005.

RESEARCH ARTICLE

The Opportunity Rover's Athena Science Investigation at Meridiani Planum, Mars

S. W. Squyres,[1]* R. E. Arvidson,[2] J. F. Bell III,[1] J. Brückner,[3] N. A. Cabrol,[4] W. Calvin,[5] M. H. Carr,[6] P. R. Christensen,[7] B. C. Clark,[8] L. Crumpler,[9] D. J. Des Marais,[10] C. d'Uston,[11] T. Economou,[12] J. Farmer,[7] W. Farrand,[13] W. Folkner,[14] M. Golombek,[14] S. Gorevan,[15] J. A. Grant,[16] R. Greeley,[7] J. Grotzinger,[17] L. Haskin,[2] K. E. Herkenhoff,[18] S. Hviid,[19] J. Johnson,[18] G. Klingelhöfer,[20] A. H. Knoll,[21] G. Landis,[22] M. Lemmon,[23] R. Li,[24] M. B. Madsen,[25] M. C. Malin,[26] S. M. McLennan,[27] H. Y. McSween,[28] D. W. Ming,[29] J. Moersch,[28] R. V. Morris,[29] T. Parker,[14] J. W. Rice Jr.,[7] L. Richter,[30] R. Rieder,[3] M. Sims,[10] M. Smith,[31] P. Smith,[32] L. A. Soderblom,[18] R. Sullivan,[1] H. Wänke,[3] T. Wdowiak,[33] M. Wolff,[34] A. Yen[14]

The Mars Exploration Rover Opportunity has investigated the landing site in Eagle crater and the nearby plains within Meridiani Planum. The soils consist of fine-grained basaltic sand and a surface lag of hematite-rich spherules, spherule fragments, and other granules. Wind ripples are common. Underlying the thin soil layer, and exposed within small impact craters and troughs, are flat-lying sedimentary rocks. These rocks are finely laminated, are rich in sulfur, and contain abundant sulfate salts. Small-scale cross-lamination in some locations provides evidence for deposition in flowing liquid water. We interpret the rocks to be a mixture of chemical and siliciclastic sediments formed by episodic inundation by shallow surface water, followed by evaporation, exposure, and desiccation. Hematite-rich spherules are embedded in the rock and eroding from them. We interpret these spherules to be concretions formed by postdepositional diagenesis, again involving liquid water.

The Mars Exploration Rover Opportunity landed in Eagle crater on Meridiani Planum on 24 January 2004 UTC, 21 days after the landing of Spirit at Gusev crater (*1*). Both vehicles landed using a variant of the airbag landing system that was developed for Mars Pathfinder, deploying the rovers after the landers had come to rest on the surface (*2*). The primary scientific objective of their mission is to explore two sites on the martian surface where water may once have been present, and to assess past environmental conditions at those sites, including their suitability for life. Here we provide an overview of the results from the 90-sol (*3*) nominal mission of Opportunity.

Like Spirit, Opportunity carries the Athena science payload (*4*). The topography, morphology, and mineralogy of the scene around the rover are revealed by a panoramic camera [Pancam (*5*)] and a miniature thermal emission spectrometer [Mini-TES (*6*)]. Both instruments view the scene using a mast (*4*) at a height of about 1.5 m above the ground. The payload also includes a 5-degree-of-freedom robotic arm (*4*). The arm carries an Alpha Particle X-ray Spectrometer [APXS (*7*)] that measures elemental abundances of rocks and soils and a Mössbauer Spectrometer (*8*) that determines the mineralogy and oxidation state of Fe-bearing phases. It also carries a Microscopic Imager [MI (*9*)] that is used to obtain high-resolution (30 μm per pixel) images of rock and soil surfaces (*10*) and a Rock Abrasion Tool [RAT (*11*)] that can remove up to ~5 mm of material over a circular area 45 mm in diameter. Finally, the payload includes seven magnets that attract fine-grained magnetic materials and can be viewed by payload instruments (*12*).

The rover itself uses a six-wheel rocker-bogie suspension system and onboard autonomous navigation and hazard avoidance capability, allowing traverse distances of tens of meters per sol (*2*). Navigation and hazard avoidance are aided by two monochromatic navigation cameras (Navcams) mounted on the mast and by four hazard avoidance cameras (Hazcams) mounted in fore- and aft-facing stereo pairs on the rover body (*13*).

The Meridiani Planum landing site (*14*) was chosen for Opportunity because its smooth flat topography would favor a safe landing and because Mars Global Surveyor TES data showed it to contain ~15 to 20% (by fractional area) of the mineral hematite (*15*). Hematite can form by a number of processes, many of which involve the action of liquid water. Orbital images showed that the hematite-bearing unit is the top stratum of a layered sequence about 600 m thick that overlies Noachian cratered terrain (*16–18*). We landed on this sequence with the hope that the hematite was an indicator that aqueous processes had been involved in its formation.

The Rover traverse. Opportunity touched down in the eastern portion of the Meridiani Planum landing ellipse (Plate 5) in an impact crater 20 m in diameter that we named Eagle crater (*19*). The landing site is named the Challenger Memorial Station (*20*). Its location in inertial coordinates was determined by fitting direct-to-Earth two-way

[1]Department of Astronomy, Space Sciences Building, Cornell University, Ithaca, NY 14853, USA. [2]Department of Earth and Planetary Sciences, Washington University, St. Louis, MO 63130, USA. [3]Max Planck Institut für Chemie, Kosmochemie, Mainz, Germany. [4]NASA Ames Research Center/SETI Institute, Moffett Field, CA 94035, USA. [5]Department of Geological Sciences, University of Nevada, Reno, NV 89557, USA. [6]U.S. Geological Survey, Menlo Park, CA 94025, USA. [7]Department of Geological Sciences, Arizona State University, Tempe, AZ 85287, USA. [8]Lockheed Martin Corporation, Littleton, CO 80127, USA. [9]New Mexico Museum of Natural History and Science, Albuquerque, NM 87104, USA. [10]NASA Ames Research Center, Moffett Field, CA 94035, USA. [11]Centre d'Etude Spatiale des Rayonnements, Toulouse, France. [12]Enrico Fermi Institute, University of Chicago, Chicago, IL 60637, USA. [13]Space Science Institute, Boulder, CO 80301, USA. [14]Jet Propulsion Laboratory, California Institute of Technology, Pasadena, CA 91109, USA. [15]Honeybee Robotics, New York, NY 10012, USA. [16]Center for Earth and Planetary Studies, Smithsonian Institution, Washington, DC 20560, USA. [17]Department of Earth, Atmospheric, and Planetary Sciences, Massachusetts Institute of Technology, Cambridge, MA 02139, USA. [18]U.S. Geological Survey, Flagstaff, AZ 86001, USA. [19]Max Planck Institut für Aeronomie, Katlenburg-Lindau, Germany. [20]Johannes Gutenberg-University, Mainz, Germany. [21]Botanical Museum, Harvard University, Cambridge MA 02138, USA. [22]NASA Glenn Research Center, Cleveland, OH 44135, USA. [23]Department of Atmospheric Sciences, Texas A&M University, College Station, TX 77843, USA. [24]Department of Civil and Environmental Engineering and Geodetic Science, Ohio State University, Columbus, OH 43210, USA. [25]Niels Bohr Institute, Ørsted Laboratory, Copenhagen, Denmark. [26]Malin Space Science Systems, San Diego, CA 92191, USA. [27]Department of Geosciences, State University of New York, Stony Brook, NY 11794, USA. [28]Department of Earth and Planetary Sciences, University of Tennessee, Knoxville, TN 37996, USA. [29]NASA Johnson Space Center, Houston, TX 77058, USA. [30]DLR Institute of Space Simulation, Cologne, Germany. [31]NASA Goddard Space Flight Center, Greenbelt, MD 20771, USA. [32]Lunar and Planetary Laboratory, University of Arizona, Tucson, AZ 85721, USA. [33]Department of Physics, University of Alabama at Birmingham, Birmingham, AL 35294, USA. [34]Space Science Institute, Martinez, GA 30907, USA.

*To whom correspondence should be addressed. E-mail: squyres@astro.cornell.edu

X-band Doppler radio transmissions and two passes of UHF two-way Doppler between Opportunity and Mars Odyssey. The lander location is 1.9483°S, 354.47417°E based on analyses of these data, translated to Mars Orbiter Laser Altimeter (MOLA)–based International Astronomical Union 2000 coordinates. The lander is located at 1.9462°S, 354.4734°E based on analyses of horizon features seen in panoramas and also observed in Mars Global Surveyor Mars Orbiter Camera (MOC) images.

Early Navcam images of the site (Fig. 1) revealed that the surface around the lander consisted of dark, fine-grained soil. Less than 10 m away from the lander was an exposure of layered bedrock in the slope of the crater wall. Egress from the lander took place on sol 7. Post-egress investigation of the soil adjacent to the lander showed it to be sprinkled with small spherules, typically 4 to 6 mm in diameter. (These spherules have become known informally as "blueberries" although their color is gray rather than blue.) On sol 14, we approached the outcrop at its closest point to the lander, a location we named Stone Mountain. Pancam and MI images showed that the spherules were weathering out of the outcrop, and APXS measurements revealed that the sulfur content of the outcrop was high. Mössbauer results suggested that the sulfate mineral jarosite was present, and Mini-TES results indicated the presence of Mg and Ca sulfates. Sols 16 to 19 were spent driving along the exposed outcrop, acquiring Pancam images for use in planning future activities. This was followed on sol 23 by use of the rover wheels to excavate a trench in soil on the crater floor and subsequent investigation of the interior of the trench. On sol 26, we drove the rover to a portion of the rock outcrop called El Capitan that we had identified in the images acquired during sols 16 to 19. Sols 27 to 36 were spent on detailed investigation of the targets Guadalupe and McKittrick on El Capitan and yielded compositional and textural evidence that liquid water had been involved in the formation and diagenesis of the outcrop rock.

On sols 37 and 38, we drove the rover to another portion of the outcrop called Last Chance that we had also identified in the images from sols 16 to 19. Detailed MI imaging of Last Chance on sols 39 and 40 and of another nearby rock called The Dells on sol 41 revealed small-scale ripple cross-lamination that provided evidence that these rocks had been deposited in flowing liquid water. The remaining sols in Eagle crater were spent investigating spherules and soil and showed that the spherules are the primary carriers of hematite at the site.

We drove Opportunity out of Eagle crater on sol 57 to begin a traverse to a much larger nearby crater named Endurance. On sols 64 to 69, we investigated an unusual basaltic rock called Bounce Rock just beyond the rim of the crater. The traverse to Endurance included a stop at a shallow trough called Anatolia (sols 70 to 72), excavation of another trench that cut through an eolian ripple (sol 73), and a stop at a 9-m impact crater called Fram (sols 85 to 88). The longest single-sol traverse, on sol 82, was 140 m. The 90-sol nominal mission ended with Opportunity ~200 m from the rim of Endurance crater and in excellent health. The total traverse distance over the nominal mission was 812 m.

Engineering data from the rover's mobility system were used to characterize materials along the traverse. Slippage during upslope traverses of soil slopes gentler than 10° in Eagle crater was less than 20% but increased rapidly with increasing slope angles (*21*), reaching a maximum of 100% on the first attempt to exit Eagle crater. Slip values are consistent with engineering testbed experience for a rover traveling over dry, loose, poorly sorted sand. Profiles retrieved from engineering data for the long traverse across the plains on sol 82 show standard deviations of the measured elevations of only 3.2 cm over the first 55 m and 40.3 cm over the total traverse distance of 140 m, which is consistent with standard deviations in elevation for Meridiani Planum determined using data from the Mars Global Surveyor MOLA instrument.

Soils. Soils at the landing site (*22*) are dominated by fine-grained basaltic sands, mixed with minor amounts of dust that is derived locally from sulfate-rich outcrops as well as globally from airfall. The first soil analyzed in Eagle crater, called Tarmac, is typical, composed of dark fine-grained olivine basalt sand with ~10% of the Fe present as hematite (*23*, *24*). MI images show the sand to be well sorted, with a mean grain size in the range of 50 to 150 μm (*25*), the size most easily moved by saltation on Mars.

Hematite in the soil is concentrated in spherules and their fragments, which are abundant on nearly all soil surfaces (Fig. 2). The abundance of hematite in Mini-TES data shows significant lateral variability (Plate 3), and the hematite abundance correlates with the abundance of spherules on the surface (*26*). Several trenches excavated using the rover wheels (Plates 14 and 15) showed that the subsurface is dominated by basaltic sand,

Fig. 1. The first image of the martian surface acquired by Opportunity. It is a Navcam image acquired on sol 1, reduced in resolution to 512 × 512 pixels and obtained before deployment of the Pancam Mast Assembly. (Image ID = 1N128285132.)

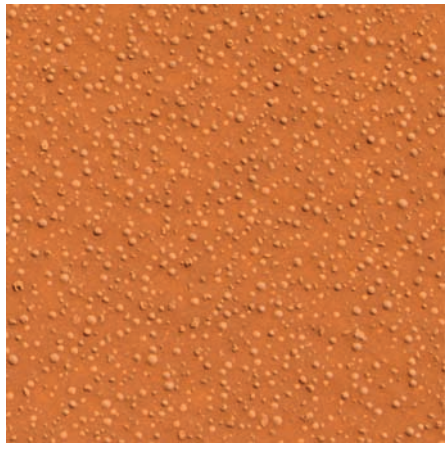

Fig. 2. Pancam image of Meridiani soil, showing a typical concentration of spherules and spherule fragments. Scale across the image is about 25 cm. This is an approximate true-color image, assembled using all of Pancam's left-eye filters. It is a 512 × 512–pixel subframe, acquired at 13:30 local solar time on sol 54.

with a much lower abundance of spherules than at the surface (*21*). The surface concentration of spherules and spherule fragments therefore constitutes a thin lag deposit or pavement. Irregular and in some cases vesicular lithic fragments, which may be basaltic, also occur in these surface concentrations.

Pancam multispectral images of soil clasts at the Opportunity landing site exhibit greater variability in reflectance spectral properties (0.4 to 1.0 μm) than previously observed in data collected from the martian surface, whether from orbit or from Earth (*27*). Spherules in particular exhibit a range of spectral properties. As spherules are exhumed from the soil by wind, some emerge with coatings that have distinct spectral characteristics. These coatings may have formed while the spherules resided in the uppermost few millimeters of the soil, where sulfates and/or other salts became cemented onto their surfaces.

Images of wheel tracks and impressions made by the Mössbauer spectrometer contact plate indicate that the soils are cohesive, with the fine-grained component filling voids between larger grains during remolding of the soils. Motor currents associated with soil trenching operations show that soils are more easily excavated at Meridiani Planum than at the Spirit landing site in Gusev crater (*21*).

At several locations along the rover's traverse, sulfate-rich bedrock outcrops are covered by no more than a meter or so of soil. Examples include immediately outside Eagle crater, near the troughs at Anatolia, and at Fram crater. In other places, the soil is thinly draped over underlying blocks of sulfate-rich rock. These observations suggest that the soils that blanket the plains are typically no more than 1 or 2 m thick, underlain everywhere by sulfate-rich rock. Because spherules are sparsely distributed in the soil, concentrated primarily at the surface, the total inventory of spherules in the soil may be the equivalent of a region-wide layer of spherules no more than a centimeter thick. The observed concentration of spherules in the underlying rock is about 1 to 2% by volume (*28*), so only about 1 m of rock needs to have been eroded away to produce all of the spherules observed in the soil.

Eolian processes. Wind at the Opportunity landing site has eroded rock, sorted soil particles during transport, formed and changed ubiquitous ripples on the plains as well as ripples and dunes in craters and troughs, and formed wind streaks seen from orbit in MOC images. Saltation of fine-grained basaltic sand has been a particularly important eolian process, abrading clasts and outcrop rock and generating impact ripples.

The plains are dominated by low ripples extending to the horizon in all directions (Fig. 3). Ripples are typically ~1 cm high, although slightly larger examples are found rimming depressions such as Eagle crater and the Anatolia trough system. The surfaces of the ripples are dominated by fragments of hematite-rich spherules. Trenching through a ripple (Plate 15) revealed induration and a substantial fraction of sand in the ripple interior (*21*) but no internal stratification. Surfaces between ripples are relatively flat, with a mixture of sand, partly buried spherule fragments, and a scattering of generally well-perched spherules. Ripple formation probably involved transport of millimeter-sized grains, either driven across the surface by saltation-induced creep or rolled directly by the wind. Individual plains ripples are oriented about 26° east of north but commonly are grouped en echelon into alignments along a secondary orientation of about 4° east of north, preserving evidence for reorientation from a clockwise change in wind direction.

Fig. 3. En echelon wind ripples on the Meridiani plains, with rover tracks (each 16 cm wide) for scale. Navcam image acquired on sol 70. (Image ID = 1N134401857.)

Ripples similar to those on the plains are seen on the southwest interior wall of Eagle crater, but otherwise the bedforms inside depressions are different. Immediately adjacent to the Challenger Memorial Station within Eagle crater is a patch of ripples composed of very fine dark sand (Plate 16). Similar ripples are seen in patches within the Anatolia troughs and Fram crater. The ripples on the floor of Eagle crater are oriented about 38° east of north. This direction is consistent with transverse motion driven by the same winds that are responsible for a bright wind streak, visible in MOC images, that extends southeast downwind from Eagle crater, supporting the notion that these sands were mobilized by the same winds that produced the streak. APXS and Mössbauer measurements on soils outside the crater that lie within the wind streak indicate that the composition of the bright material is consistent with airfall dust (*23*, *24*), preserved in protected areas immediately downwind from the crater.

Small tails of sculpted rock extend from some spherules that lie partially embedded within and protruding from some rocks and indicate erosion of these rocks due to saltating particles driven by strong unidirectional winds. No dunes were observed during the 90-sol nominal mission, but dunes were subsequently discovered on the floor of Endurance crater.

Bedrock outcrops. The bedrock outcrop in Eagle crater (Plate 13) is 30 to 50 cm high and is exposed in an arc that subtends nearly 180 degrees of the crater wall, centered on its northwest quadrant. Brecciation associated with the impact crater has disrupted the stratigraphy. The dominant physical characteristic of the rock is fine lamination on scales of a few millimeters (Fig. 4). The outcrop can be subdivided and mapped into several distinct units based on its color, morphology, texture, and structural attitude (*28*).

The rock composing the outcrop is physically weak compared to some other rocks on Mars. The energy required to grind it with the RAT is 30 to 50 times lower per unit of volume than for the basaltic rocks investigated at Gusev crater by Spirit (*21*). The greatest resistance to grinding within the outcrop is found on the steepest slopes: The more resistant target Guadalupe is located on a 36° slope whereas the less resistant target McKittrick is located on a 7° slope, consistent with the idea that harder rocks retain steeper slopes because they are more resistant to erosion.

At a microscopic scale (*25*), four primary physical constituents are seen in the rock. The dominant one is medium to coarse sand grains, which tend to be well sorted within individual laminae. The second is the gray spherules, typically 4 to 6 mm in diameter, that are embedded within the rock (Plates 7, 9, and 10) with a spatial distribution that is more uniform than random. The third is fine-grained cement that binds the sand grains, and the fourth is small tabular vugs (Plate 9) that crosscut the laminations at random orientations.

The rock has a high concentration of sulfur, with up to about 25 weight percent SO_3 found in some locations (*23*). Much of the sulfur may be present in sulfate salts. The Mössbauer spectrometer has detected the Fe sulfate jarosite in all exposures of the outcrop that we have investigated (*24*). Mini-TES spectra of the outcrop also indicate that Mg and Ca sulfates are present at levels of a few tens of percent (*26*), although jarosite is below the Mini-TES detection limit. Chlorine and bromine are also detected by the APXS, and the Cl/Br ratio of the rock varies by more than an order of magnitude over small length scales (*23*).

The spherules are different in chemistry from the rock in which they are embedded. Based on Mössbauer and APXS data (*24*, *23*), we estimate that the spherules are more than 50% hematite by mass. Because of this composition, their spatial distribution, and several distinctive aspects of their morphology (*28*), we interpret the spherules to be concretions that formed by precipitation from aqueous fluids within the rock sometime after the sediments were deposited. The vugs are interpreted to represent crystal molds (*29*) formed by dissolution of one or more soluble mineral phases, possibly sulfates.

At several locations, the laminations within the rock exhibit cross-stratification (*28*). Some cross-bed sets may have resulted from eolian processes, but others show a small-scale festoon geometry indicating transport in subaqueous ripples (Plates 6 and 7). The three-dimensional geometry required by such cross-stratification implies that the ripples had highly sinuous crestlines with characteristic length scales of a few centimeters, a geometry that is indicative of transport by gently flowing water (*30*–*32*).

Rocks with these characteristics are not limited to Eagle crater. Rocks with similar properties were also observed within the Anatolia troughs (Fig. 5), although the rover was unable to approach the rocks there because of safety concerns, and the origin of the troughs remains enigmatic. Similar rocks were also observed at Fram crater (Plate 4), and there we made measurements with all the in situ instruments that confirmed that the rocks are virtually identical in composition, texture, and spherule content to ones observed at Eagle crater. We can therefore infer that sulfate-dominated sedimentary rocks extend laterally over a length scale of at least half a kilometer at the Opportunity landing site.

Bounce Rock. About 20 m beyond the rim of Eagle crater, we encountered a solitary rock about 40 cm across that we named Bounce Rock because of its proximity to an airbag bounce mark (Plate 12). The composition of Bounce Rock is unique at the Meridiani site and is also distinct from any material observed at Gusev crater by Spirit. The Mössbauer spectrum of Bounce Rock shows only pyroxene, with no other Fe-bearing minerals present in detectable quantities (*24*). The APXS chemistry is basaltic, with a normative mineralogy dominated by pyroxene and plagioclase and lacking in olivine (*23*). In both its mineralogy and chemistry, Bounce Rock is similar to Lithology B of the shergottite meteorite EETA79001 (*33*). In MI images it exhibits a rough and largely aphanitic texture, with some features suggestive of brecciation (*25*). Despite the basaltic composition, grinding with the RAT shows that it is weak and friable, with a grinding energy per unit of volume of 3.7 J/mm^3, almost an order of magnitude lower than is typical of fresh basalts at Gusev crater (*21*).

These distinct characteristics of Bounce Rock, together with its isolated occurrence, suggest that it may not be locally derived. A possible source for this enigmatic rock is a relatively fresh 25-km crater located 75 km southwest of Eagle crater, whose continuous ejecta lies atop the hematite-bearing plains (*34*). Rays of blocky material from this crater are observed within 10 km of Eagle crater in Mars Odyssey Thermal Emission Imaging System nighttime images (*35*), indicating that material from this crater was deposited on the current surface of Meridiani Planum in the vicinity of Eagle crater. The weak friable nature of Bounce Rock is consistent with a history involving impact shock and ballistic transport. A 25-km crater samples to depths of several kilometers, suggesting that Bounce Rock may represent materials from the older volcanic plains that have been interpreted to underlie the layered unit of the Meridiani Formation (*17*, *18*, *34*, *35*). In this case, these lower units are compositionally distinct from the basaltic sands that cover the plains around Eagle crater.

Atmospheric science. In addition to our geologic investigations, the remote sensing instruments on the payload have been used to observe the martian atmosphere. Upward-looking Mini-TES spectra are diagnostic of the vertical thermal structure of the atmosphere between about 20 m and 2 km above the surface, column-integrated infrared aerosol optical depth and water vapor abundance, and aerosol particle size. In particular, temperature profiles retrieved from Mini-TES observations of the 15-μm absorption band of CO_2 provide systematic characterization of the martian boundary layer (*36*). These observations show the development of a near-surface superadiabatic layer during the afternoon and a deep inversion layer at night. Upward-looking Mini-TES "stares," in which spectra are collected every 2 s for up to an hour, show warm and cool parcels of air moving through the Mini-TES field of view on a time scale of 30 s. Dust properties are consistent with previous measurements; spe-

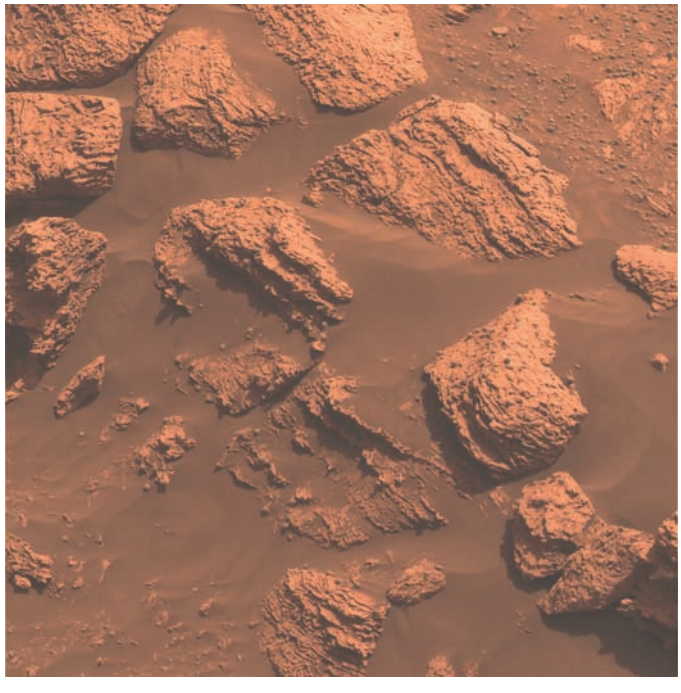

Fig. 4. Pancam image showing fine-scale laminations in the Eagle crater outcrop. Scale across the image is about 60 cm. This is an approximate true-color image, assembled using images from the 480-, 540-, and 600-nm filters. It was acquired at about 11:00 local solar time on sol 14.

cifically, cross-section mean radius is 1.5 ± 0.2 μm.

Pancam and Mini-TES observations of aerosols have been used to monitor the fallout of dust after a large regional dust storm that occurred in December 2003 and the further clearing associated with the transition into the southern hemisphere fall season (*37*). Direct solar imaging using Pancam with the 440/880-nm neutral density filters provides an accurate measurement of visible-wavelength aerosol optical depth. Visible-wavelength dust optical depth at the Meridiani Planum landing site dropped from a value of 0.90 soon after landing to about 0.6 on sol 91 (*38*).

Atmospheric dust transport can also be investigated by study of dust buildup rates on rover surfaces, particularly solar cells (*21*). Analyses of short-circuit current monitor solar cell data show a decrease in current of 0.29% per sol (corrected for seasonal variations in Mars-Sun distance and solar elevation angle) during the first 25 sols of the mission, slowing to 0.13% per sol by sol 90. Given the low surface albedo, high winds must remove dust deposits on a frequent basis, thereby keeping the surface relatively free of dust.

Evolution of Meridiani Planum. The Opportunity landing site is underlain by flat-lying sedimentary rocks. We interpret these rocks to be a mixture of chemical and siliciclastic sediments with a complex diagenetic history (*28*). The environmental conditions that they record are episodic inundation by shallow surface water, followed by evaporation, exposure, and desiccation. Our data suggest that the sediments are, by weight, ~50% fine-grained siliciclastic materials derived from weathering of basaltic parent rocks, ~40% sulfate minerals, and ~10% hematite. After deposition, hematite-rich concretions grew by precipitation from groundwater, and tabular mineral grains, probably sulfates, grew and were subsequently removed to produce the vugs. Some concretions were later eroded from the rock by eolian processes and are now concentrated in near-surface soils, producing the strong hematite signal seen from orbit.

The aqueous history recorded in these rocks may be characteristic of a large geographic region. MOC images show that a relatively high-albedo unit that correlates with the outcrop exposures near the Opportunity landing site is at least discontinuously present across most of Meridiani Planum. It seems likely, then, that the area over which these aqueous processes operated was at least tens of thousands of square kilometers in size.

The timing of the sedimentation is more difficult to determine. An upper bound on the age can be derived from analyses of orbital images that show that the Meridiani plains materials disconformably overlie dissected Middle to Late Noachian cratered terrains (*39*), suggesting that the sedimentary rocks at the Opportunity site could be as much as several billion years old.

Sometime after the end of aqueous activity at Meridiani, a thin layer of fine-grained basaltic sand was deposited atop the sedimentary rocks. The source of this sand cannot be determined from our data. One possibility is that it was excavated by impacts from units that underlie the sulfate-rich sediments, but we have been unable to identify such units in our traverse to date. Ejecta of Eagle, Fram, and Endurance craters do not show obvious strewn fields of basaltic rock fragments, so we presently have no good evidence for any basaltic rock immediately beneath the sulfate-rich sediments. And although Bounce Rock is a basalt, its pyroxene-dominated composition differs from that of the sand.

Another possible origin for the sand is that it is the erosional remnant of some overlying unit that has now been mostly removed. To the extent that superjacent, poorly consolidated strata were stripped away by erosion, the upper surface of the sulfate-rich sediments would seem to have created a barrier to continuing sediment removal. However, no evidence of former overlying units has emerged in the traverse to date either. Indeed, the flat surface of Meridiani Planum and the lack of erosional remnants of stratigraphically higher units suggest that the current plains surface may effectively represent the original depositional top of the entire sedimentary sequence. If the basaltic sand is neither excavated from below the sulfate-rich sediments nor the remnants of a former overlying unit, then perhaps it was transported by saltation from adjacent regions.

Regardless of the origin of the thin surface layer of sand, the underlying sulfate-rich sedimentary rocks at Meridiani Planum clearly preserve a record of environmental conditions different from any on Mars today. Liquid water was once present intermittently at the martian surface at Meridiani, and at times it saturated the subsurface. Because liquid water is a key prerequisite for life, we infer that conditions at Meridiani may have been habitable for some period of time in martian history.

Fig. 5. The Anatolia trough system. Portion of a Navcam mosaic obtained at about 12:30 local solar time on sol 74.

References and Notes

1. S. Squyres *et al.*, *Science* **305**, 794 (2004).
2. J. A. Crisp *et al.*, *J. Geophys. Res.* **108**, 8061 (2003).
3. A martian solar day has a mean period of 24 hours 39 min 35.244 s and is referred to as a sol to distinguish it from a ~3% shorter solar day on Earth.
4. S. W. Squyres *et al.*, *J. Geophys. Res.* **108**, 8062 (2003).
5. J. F. Bell III *et al.*, *J. Geophys. Res.* **108**, 8063 (2003).
6. P. R. Christensen *et al.*, *J. Geophys. Res.* **108**, 8064 (2003).
7. R. Rieder *et al.*, *J. Geophys. Res.* **108**, 8066 (2003).
8. G. Klingelhöfer *et al.*, *J. Geophys. Res.* **108**, 8067 (2003).
9. K. E. Herkenhoff *et al.*, *J. Geophys. Res.* **108**, 8065 (2003).
10. The term martian soil is used here to denote any loose, unconsolidated materials that can be distinguished from rocks, bedrock, or strongly cohesive sediments. No implication of the presence or absence of organic materials or living matter is intended.
11. S. Gorevan *et al.*, *J. Geophys. Res.* **108**, 8068 (2003).
12. M. B. Madsen *et al.*, *J. Geophys. Res.* **108**, 8069 (2003).
13. J. Maki *et al.*, *J. Geophys. Res.* **108**, 8071 (2003).
14. M. P. Golombek *et al.*, *J. Geophys. Res.* **108**, 8072 (2003).
15. P. R. Christensen *et al.*, *J. Geophys. Res.* **105**, 9632 (2000).
16. B. M. Hynek and R. J. Phillips, *Geology* **29**, 407 (2001).
17. R. E. Arvidson *et al.*, *J. Geophys. Res.* **108**, 8073 (2003).
18. B. M. Hynek, R. E. Arvidson, R. J. Phillips, *J. Geophys. Res.* **107**, 5088 (2002).

19. Names have been assigned to geographic features by the Mars Exploration Rover (MER) team for planning and operations purposes. They are not formally recognized by the International Astronomical Union.
20. The Challenger Memorial Station was named to honor the crew of the Space Shuttle *Challenger*, who perished on 28 January 1986. The name Challenger Memorial Station refers both to the lander itself and to the martian terrain that it occupies.
21. R. E. Arvidson *et al.*, *Science* **306**, 1730 (2004).
22. L. A. Soderblom *et al.*, *Science* **306**, 1723 (2004).
23. R. Rieder *et al.*, *Science* **306**, 1746 (2004).
24. G. Klingelhöfer *et al.*, *Science* **306**, 1740 (2004).
25. K. E. Herkenhoff *et al.*, *Science* **306**, 1727 (2004).
26. P. R. Christensen *et al.*, *Science* **306**, 1733 (2004).
27. J. F. Bell III *et al.*, *Science* **306**, 1703 (2004).
28. S. W. Squyres *et al.*, *Science* **306**, 1709 (2004).
29. P. W. Choquette, L. C. Pray, *Am. Assoc. Petrol. Geol. Bull.* **54**, 207 (1970).
30. J. C. Harms, J. B. Southard, R. G. Walker, *Structures and Sequences in Clastic Rocks* (Society of Economic Paleontologists and Mineralogists, Tulsa, OK, 1982).
31. G. V. Middleton, J. B. Southard, *Mechanics of Sediment Movement* (Society of Economic Paleontologists and Mineralogists, Providence, RI, 1984).
32. J. B. Southard, J. A. Boguchwal, *J. Sed. Petrol.* **66**, 680 (1990).
33. A. Banin, B. C. Clark, H. Wänke, in *Mars*, H. H. Kieffer, B. M. Jakosky, C. W. Snyder, M. S. Matthews, Eds. (Univ. of Arizona Press, Tucson, AZ, 1992), pp. 584–625.
34. P. R. Christensen, R. V. Morris, M. D. Lane, J. L. Bandfield, M. C. Malin, *J. Geophys. Res.* **106**, 23 (2001).
35. P. R. Christensen, S. W. Ruff, *J. Geophys. Res.* **109**, E08003 (2004).
36. M. D. Smith *et al.*, *Science* **306**, 1750 (2004).
37. M. D. Smith, *Icarus* **167**, 148 (2004).
38. M. T. Lemmon *et al.*, *Science* **306**, 1753 (2004).
39. R. E. Arvidson *et al.*, *J. Geophys. Res.* **108**, 8073 (2003).
40. We are deeply indebted to the many hundreds of engineers and scientists—far too numerous to name here—who made the MER Project and the Athena Science Investigation possible. Funding for the MER Project, including most of the Athena Payload, was provided by NASA. The APXS and Mössbauer instruments were funded by the German space agency (DLR), and the magnet array was funded by the Danish government. A portion of the research described in this paper was carried out at the Jet Propulsion Laboratory, California Institute of Technology, under a contract with NASA. The MER Project was led with skill and dedication by P. Theisinger, and the development of the MER flight system was led with equal skill and dedication by R. Cook and B. Goldstein. J. Rademacher managed the development of the Mini-TES, APXS, and Mössbauer payload elements, M. Schwochert led the engineering teams for Pancam and the Microscopic Imager, and S. Kondos and M. Johnson managed the development of the RAT. To all of them, and to the hundreds of members of the MER family who have made this adventure such a joy and privilege to be part of, we express our heartfelt and lasting thanks.

Plates Referenced in Article

www.sciencemag.org/cgi/content/full/306/5702/1698/DC1

Plates 3 to 7, 9, 10, and 12 to 16

7 October 2004; accepted 2 November 2004

RESEARCH ARTICLE

Pancam Multispectral Imaging Results from the Opportunity Rover at Meridiani Planum

J. F. Bell III,[1]* S. W. Squyres,[1] R. E. Arvidson,[2] H. M. Arneson,[1] D. Bass,[3] W. Calvin,[4] W. H. Farrand,[5] W. Goetz,[6] M. Golombek,[3] R. Greeley,[7] J. Grotzinger,[8] E. Guinness,[2] A. G. Hayes,[1] M. Y. H. Hubbard,[1] K. E. Herkenhoff,[9] M. J. Johnson,[1] J. R. Johnson,[9] J. Joseph,[1] K. M. Kinch,[10] M. T. Lemmon,[11] R. Li,[12] M. B. Madsen,[6] J. N. Maki,[3] M. Malin,[13] E. McCartney,[1] S. McLennan,[14] H. Y. McSween Jr.,[15] D. W. Ming,[16] R. V. Morris,[16] E. Z. Noe Dobrea,[1] T. J. Parker,[3] J. Proton,[1] J. W. Rice Jr.,[7] F. Seelos,[2] J. M. Soderblom,[1] L. A. Soderblom,[9] J. N. Sohl-Dickstein,[1] R. J. Sullivan,[1] C. M. Weitz,[17] M. J. Wolff[5]

Panoramic Camera (Pancam) images from Meridiani Planum reveal a low-albedo, generally flat, and relatively rock-free surface. Within and around impact craters and fractures, laminated outcrop rocks with higher albedo are observed. Fine-grained materials include dark sand, bright ferric iron–rich dust, angular rock clasts, and millimeter-size spheroidal granules that are eroding out of the laminated rocks. Spectra of sand, clasts, and one dark plains rock are consistent with mafic silicates such as pyroxene and olivine. Spectra of both the spherules and the laminated outcrop materials indicate the presence of crystalline ferric oxides or oxyhydroxides. Atmospheric observations show a steady decline in dust opacity during the mission. Astronomical observations captured solar transits by Phobos and Deimos and time-lapse observations of sunsets.

On 24 January 2004 UTC, the Mars Exploration Rover Opportunity landed on Mars within the classical low-albedo Noachian terrain of Meridiani Planum. The landing region was previously identified in orbital remote sensing data as being flat-lying layered and/or etched materials characterized by an unusual surficial concentration of coarse-grained gray hematite at the 15 to 20% areal abundance level (*1*–*3*). The lander and encapsulated rover came to rest inside an impact crater, 3 m deep and 20 m in diameter, informally known as Eagle crater (*4*). Using the Pancam charge-coupled device (CCD) imaging system (*5*, *6*), we acquired high spatial resolution multispectral panoramic images of the landing site and its environs to characterize the morphology, composition, and physical and atmospheric properties of the region.

Pancam images were calibrated using preflight laboratory measurements and then converted to *I/F* (where I = measured scene radiance and πF = the solar irradiance at the top of the martian atmosphere), which is reflectance relative to the onboard Pancam calibration target, corrected for solar incidence angle and dust deposition effects (*5*–*7*). During Opportunity's 90-sol primary mission, more than 8900 Pancam images were acquired and downlinked. These images include two 360° 5- and 6-color stereo panoramas from inside Eagle crater and on the plains just outside the crater, four 7-color stereo mosaics covering the Eagle crater outcrop at high resolution, more than 100 11-color multispectral spot observations of trenches, Rock Abrasion Tool (RAT) drill holes and other rock and soil (*8*, *9*) regions of interest within Eagle crater and during the traverse across the plains, and photometric imaging sequences designed to

[1]Department of Astronomy, Cornell University, Ithaca NY 14853, USA. [2]Department of Earth and Planetary Sciences, Washington University, St. Louis, MO 63130, USA. [3]Jet Propulsion Laboratory, California Institute of Technology, Pasadena, CA 91109, USA. [4]Department of Geological Sciences, University of Nevada, Reno, NV 89501, USA. [5]Space Science Institute, Boulder, CO 80301, USA. [6]University of Copenhagen, DK-2100 Copenhagen Ø, Denmark. [7]Department of Geological Sciences, Arizona State University, Tempe, AZ 85287, USA. [8]Department of Earth, Atmospheric, and Planetary Sciences, Massachusetts Institute of Technology, Cambridge, MA 02139, USA. [9]U.S. Geological Survey, Flagstaff, AZ 86001, USA. [10]Aarhus University, DK-8000 Aarhus C, Denmark. [11]Department of Atmospheric Sciences, Texas A&M University, College Station, TX 77843, USA. [12]Department of Civil and Environmental Engineering and Geodetic Science, Ohio State University, Columbus, OH 43210, USA. [13]Malin Space Science Systems Inc., San Diego, CA 92191, USA. [14]Department of Geosciences, State University of New York, Stony Brook, NY 11794, USA. [15]Department of Earth and Planetary Sciences, University of Tennessee, Knoxville, TN 37996, USA. [16]NASA Johnson Space Center, Houston, TX 77058, USA. [17]Planetary Science Institute, Tucson, AZ 85719, USA.

*To whom correspondence should be addressed. E-mail: jfb8@cornell.edu